Atmos. Chem. Phys. Discuss., 11, 29251–29282, 2011
www.atmos-chem-phys-discuss.net/11/29251/2011/
doi:10.5194/acpd-11-29251-2011

Atmospheric Chemistry and Physics Discussions

The Morning NO_x maximum in the forest atmosphere boundary layer

M. Alaghmand[1], P. B. Shepson[1,2,3], T. K. Starn[4], B. T. Jobson[5], H. W. Wallace[5], M. A. Carroll[6], S. B. Bertman[7], B. Lamb[5], S. L. Edburg[5], X. Zhou[8], E. Apel[9], D. Riemer[10], P. Stevens[11], and F. Keutsch[12]

[1]Purdue University, Dept. of Chemistry, West Lafayette, IN, USA
[2]Dept. of Earth and Atmospheric Sciences, West Lafayette, IN, USA
[3]Purdue Climate Change Research Center, West Lafayette, IN, USA
[4]West Chester University, Dept. of Chemistry, West Chester, PA, USA
[5]Washington State University, Dept. of Civil and Environmental Engineering, Pullman, WA, USA
[6]University of Michigan, Dept. of Atmospheric, Oceanic, and Space Sciences, Ann Arbor, MI, USA
[7]Western Michigan University, Dept. of Chemistry, Kalamazoo, MI, USA
[8]Wadsworth Center, SUNY-Albany, NY, USA
[9]National Center for Atmospheric Research, Boulder, CO, USA
[10]RSMAS, University of Miami, Miami, FL, USA

[11]Indiana University, School of Public and Environmental Affairs, Bloomington, IN, USA
[12]University of Wisconsin, Madison, Dept. of Chemistry, Madison, WI, USA

Received: 22 August 2011 – Accepted: 11 October 2011 – Published: 28 October 2011

Correspondence to: P. B. Shepson (pshepson@purdue.edu)

Published by Copernicus Publications on behalf of the European Geosciences Union.

Abstract

During the 1998, 2000, 2001, 2008, and 2009 summer intensives of the Program for Research on Oxidants: PHotochemistry, Emissions and Transport (PROPHET), ambient measurement of nitrogen oxides ($NO + NO_2 = NO_x$) were conducted. NO and NO_x mole fractions displayed a diurnal pattern with NO_x frequently highest in early morning. This pattern has often been observed in other rural areas. In this paper, we discuss the potential sources and contributing factors of the frequently observed morning pulse of NO_x. Of the possible potential contributing factors to the observed morning pulse of NO and NO_x, we find that surface-layer transport and slow upward mixing from soil emissions, related to the thermodynamic stability in the nocturnal boundary layer (NBL) before its morning breakup are the largest contributors. The morning NO_x peak can significantly impact boundary layer chemistry, e.g. through production of HONO on surfaces, and by increasing the importance of NO_3 chemistry in the morning boundary layer.

1 Introduction

A wide variety of environmental and health impacts result from the emission of NO_x ($NO + NO_2$) into the atmosphere, including acidic deposition (Galloway et al., 2008), stimulation of forest growth (Ollinger et al., 2002; Magnani et al., 2007; Lockwood et al., 2008; Costa et al., 2011), including a potentially strong impact on the atmospheric CO_2 "fertilization effect" (Norby et al., 2010), production of ozone, and altering (indirectly and directly) atmospheric aerosol concentrations. Continental atmospheric boundary layers typically have NO_x concentrations of 1–3 ppb (Parrish et al., 1993; Thornberry et al., 2001), while clean, remote locations have very low NO_x concentrations ranging between 4 and 50 ppt (Kondo et al., 1996). NO_x regulates photochemical production of tropospheric ozone, and hydroxyl and peroxy radical concentrations directly and indirectly (Lin et al., 1988; Thompson, 1992). When nitric oxide (NO) is converted to

nitrogen dioxide (NO_2) by oxidants other than ozone, such as hydroperoxyl radicals (HO_2) or organic peroxy radicals (RO_2), a net photochemical production of ozone results (Ridley et al., 1992). NO_x chemistry, in the presence of other species such as BVOCs (Rollins et al., 2010), NH_3 (Dentener and Crutzen, 1994) and humidity, produces nitric acid (HNO_3) and aerosol. Thus, through connection to ozone and aerosol production, and through impacts on the carbon cycle, nitrogen chemistry is linked to changes in climate. Understanding the sources and fate of NO_x and the distribution of odd nitrogen species is important for quantifying human impacts on both atmospheric composition and climate (Penner et al., 1991).

Since 1997 we have been conducting measurements of NO_x, O_3, VOCs, and radicals as part of the Program for Research on Oxidants: PHotochemistry, Emissions and Transport (PROPHET; Carroll et al., 2001) at the University of Michigan Biological Station, situated near the tip of the Michigan lower peninsula in a mixed deciduous/coniferous forest site. At this site, a morning NO_x peak at the sampling location above the forest canopy is routinely observed (Fig. 1). A morning NO_x peak has been observed at other surface sites that are removed from anthropogenic sources (Martin et al., 1991; Parrish et al., 1993; Thornberry et al., 2001). Parrish et al. (1993) reported that $(NO)/(NO_y)$ peaked in the early morning when NO_2 was photodissociated rapidly. Thornberry et al. (2001) hypothesized that during the breakup of the nocturnal boundary layer (NBL) in the morning, air aloft is mixed down to the surface, resulting in an increase of NO_x at the surface for sites such as PROPHET, where local emissions are small. Day et al. (2009) observed and explained a morning NO_x peak as resulting from this process. However, this hypothesis does not always explain the PROPHET observations, since the morning NO_x peak often starts before sunrise (i.e. well before the NBL breakup). In addition, there are some cases at PROPHET during which turbulence data do not support interpretation of the morning NO_x peak via downward mixing of polluted air to the surface. There are a number of possible contributors to the observed morning NO_x peak, including: photolysis of highly photo-labile substances that have deposited onto the canopy during nighttime; HONO photodissociation after its

nighttime production at the surface (Zhou et al., 2011); downward mixing of polluted air from the residual layer to the surface when the NBL breaks up; local scale combustion; long-range transport of polluted air; and soil NO_x emission. Here, we set out to evaluate these possibilities to identify the underlying cause of this phenomenon and discuss the supporting data and implications. This study leverages a range of observations from the University of Michigan Biological Station PROPHET tower site (Carroll et al., 2001) over a number of different growing seasons.

2 Experimental

Field studies with relevant and supporting data were conducted in the summers of 1998, 2000, 2001, 2008 and 2009 at the PROPHET measurement site (Carroll et al., 2001). This site consists of a 31.5 m tall scaffolding tower located in a rural mixed deciduous/coniferous forested area near the northern tip of the lower peninsula of Michigan (45.559° N, 84.715° W). The typical canopy height is ∼22 m and is dominated by aspen, with some maple, oak, birch, beech and a successional undergrowth of white pine (Gough et al., 2007). A range of measurements of NO_x, NO_y, PAN, O_3, aerosol, CO, VOCs, radiation, temperature and wind speed/direction are available in the PROPHET data archive. Most instrumentation was located in the PROPHET laboratory building at the base of the tower. For most instruments air was sampled from a port on the lowest segment of the common 5 cm ID Pyrex manifold that drew air from a height of 35 m into the laboratory building at the base of the tower with a residence time of < 2 s (Carroll et al., 2001). NO_x was measured using a custom-built NO chemiluminescence analyzer, constructed as described by Ridley and Grahek (1990). For the instrument used in 2008, chemiluminescence photons were detected using a Burle Industries 8852 photomultiplier tube, cooled using dry ice, and using a Hamamatsu photon counting system. The instrument incorporates a blue light LED NO_2 photolytic converter. Artifact tests (reaction of ambient air with ozone in a pre-reaction chamber) were conducted to assess the background from chemiluminescence generated by ozone reaction with other

atmospheric compounds. The artifact test was done before each ambient air sample measurement. The NO_2 converter, which has two blue light photodiodes on either end of the converter, photolyzes NO_2 to NO. The wavelength output of the photodiodes makes the converter very selective for NO_2 because interferents (e.g. HONO and NO_3) do not absorb energy in the photodiode output wavelength range. The average NO_2 conversion efficiency for a flow rate of 1.2 slpm was determined to be 28.6 ± 0.9 %. The instrument was calibrated daily by dilution of a 5.0 ppm NO in nitrogen standard (Praxair) with ultra-zero air. An independent calibration using a separate NO standard (5 ppm; Praxair) was used to evaluate the accuracy of the standards. These two standards differed by 2 %. The 3σ, 1 min avgerage detection limit for the 2008 study for NO and NO_2 was 7 ppt. In 2001, NO_x and NO_y were measured via a similar instrument, as described by Thornberry et al. (2001).

In 2009 NO and NO_2 were measured simultaneously using a 2-channel chemiluminescence instrument (Air Quality Design) with a blue light LED converter for NO_2. Sensitivity calibrations were performed daily using standard addition of 10 sccm NO calibration gas 101.4 ppmv ± 1 % NIST traceable from Scott-Marrin, Inc. The blue light NO_2 converter was calibrated by gas phase titration of the NO calibration gas to NO_2 using ozone, and the average conversion efficiency was ∼60 %. The average sensitivity was ∼4 counts per pptv and 5 counts per pptv on the NO and NO_2 channels, respectively. The background counts were 1300 for the NO channel and 1500 Hz for the NO_2 channel. The minimum detection limits defined as 3 times the standard deviation of a 60 second zero air measurement were 25 pptv for NO and 33 pptv for NO_2. Sampling was done from 3 separate PFA Teflon inlets to measure the vertical gradients through the canopy. The sampling heights were 6 m, 20 m and 34 m. The diameters of the PFA tubes were1/2″ for the 6-m and 20-m tubes and 5/8″ for the 34m tube. The flow rates were approximately 80 slpm for the 1/2″ tubes and 130 slpm for the 5/8″ tube. An automated valving system cycled a 10 min sampling duration sequentially from each inlet for approximately 3 weeks.

Benzene and toluene were measured by GC/MS, as described by Apel et al. (2002). Aerosol size distributions were measured using a Scanning Mobility Particle Sizer (SMPS), deployed on the tower at a height of 26 m, 4 m above the average canopy height. The sampling inlet consisted of 7 m of $^1/_4''$ Tygon tubing. A GAST pump was used to create a fast flow rate, while the SMPS sampled from a tee connected to the tubing that led to the pump. The flow rate of the pump was set to 1.5 L/min. using a needle valve. Size distribution data were collected every 5 minutes, continuously, except during periods of vertical profiling within the forest canopy.

A TECO 49C Ozone monitor was employed to determine ozone, with a precision of ~1 ppb. CO concentrations in 2001 were determined using a TECO 48C. PAN was determined using a GC-ECD instrument, as described in Pippin et al. (2001).

3 Results and discussion

Figure 1 presents the diurnal average (hourly) NO_x and radiation observed at the PROPHET site over the 24 June 2008 to 26 July 2008 measurement period. Figure 1S (see Supplement) shows four different daily observations. As shown in Fig. 1 there is, on average, an increase of ~1 ppb of NO_x at the tower sampling inlet (34 m, approximately 12 m above canopy height) between 03:00 to 07:00 (all times reported in EST unless noted) with a maximum around 07:00. We observe the average NO_x mole fraction to begin to increase before sunrise, as shown in individual cases below. A plot of the frequency of the time of day for the maximum in NO_x is shown in Fig. 2. While the peak occurs at 0730, there are significant numbers of events that occur with earlier maxima, when the atmosphere is still quite stable, prior to breakup of the NBL due to solar heating. For the time period 04:00–08:00, the distribution (histogram) of NO_x observations (data not shown) is very broad, with a peak at 600–800 ppt, but extending out to ~3000 ppt; in contrast, the midday distribution is rather sharp, with a peak in the 500–900 ppt range, with essentially no observations for [NO_x]> 2000 ppt (data not shown).

The increase in NO in the morning can be readily explained by photolysis of NO_2, and the photostationary state relationship (Reactions R1–3 and Eq. 1).

$$NO_2 + h\nu \rightarrow NO + O(^3P) \quad \text{(R1)}$$

$$O(^3P) + O_2 \rightarrow O_3 \quad \text{(R2)}$$

$$O_3 + NO \rightarrow NO_2 + O_2 \quad \text{(R3)}$$

$$(NO)_{pss} = J_{NO2}(NO_2)/k_3(O_3) \quad (1)$$

As an example, in Fig. 3 we show the observed (NO), along with the calculated $[NO]_{pss}$ from Eq. (1), for 1 July 2008. Figure 3 shows the calculated J_{NO2}, and observed O_3 mole fraction for that day. $[NO]_{pss}$ has the same shape and comparable magnitude as the observed [NO] in the morning, and thus photolysis of NO_2 can explain the morning NO peak. While NO_2 photolysis can explain the NO peak, it does not explain the morning NO_x peak that is often observed before sunrise. Below we discuss each of the potential mechanisms that could explain a morning NO_x peak.

3.1 HONO production and photolysis

As discussed by many in the past, HONO is produced on a variety of surfaces (Sakamaki et al., 1987; Finlayson-Pitts et al., 2003; Zhou et al., 2002, 2011), e.g. as shown in Reaction (R4). If sufficient HONO were produced on forest canopy surfaces and released to the stable boundary layer, photolysis upon sunrise (Reaction R5) could account for some of the NO_x.

$$2NO_2 + H_2O \rightarrow HNO_3 + HONO \quad \text{(R4)}$$

$$HONO + h\nu \rightarrow NO + OH \quad \text{(R5)}$$

To test this, we calculated the total possible production of NO_x from HONO photolysis for the average data, using the HONO observations for 23 July 2008; J_{HONO}[HONO]

was integrated over the period 03:35 to 07:10, during which (HONO) was 20–25 ppt, and during which NO_x increased by 611 ppt, from about 1100 ppt. Integrated HONO photolysis over this period yielded a total NO_x production of ~84 ppt, only 14 % of the observed 611 pptv increase in NO_x. We note that we used clear sky J_{HONO} values for this calculation, so our NO_x production from HONO photolysis is an upper limit. Interestingly, (HONO) increases through the morning with radiation at this site, and thus photo-induced HONO production is much more important than the dark production mechanism. Thus while HONO production and photolysis is significant (especially as an OH source), it appears to represent only a minor source of NO_x production at the surface at this site.

3.2 Downward mixing of polluted air

As discussed by Hastie et al. (1993) and others, the NBL is thermodynamically stable, with a positive lapse rate that can be as much as $0.04\,K\,m^{-1}$ (see Fig. 4, for 24 July 2008; this was a typical clear sky night, with a large NO_x peak before sunrise, see Fig. 8). The air near the surface is therefore isolated from that aloft, resulting in exponential decay in concentrations of various pollutants at the surface, due to dry depositional loss. Downward mixing of polluted (i.e. high NO_x) air from aloft (e.g. from within the residual layer, or from nocturnal jets, Singh et al., 1993), may result in an increase in [NO_x] (or other species that are relatively surface-depleted) at the surface. If this were the case, within the polluted layer aloft would be elevated concentrations of CO (if the source is combustion) as well as of PAN and O_3, relative to the surface layer at tower height due to dry depositional loss of PAN and O_3 from the surface layer during the time prior to the occurrence of the peak (Hastie et al., 1993). A viable hypothesis is that downward mixing of air either not subject to dry depositional losses, or containing transported pollution, would cause an increase of these species observed at the surface. However, we find that the data typically do not support this hypothesis. In Figs. 5–7 we show example data sets. Figure 5 shows the diurnal average of CO, NO_x and radiation observed for the summer of 2001. As shown in the figure, CO is relatively

constant at the time of the NO_x maximum, and thus inconsistent with downward mixing of polluted air. Futhermore, beginning at 08:00 (a time typically associated with the start of the NBL breakup) NO_x decreases, likely from dilution with relatively cleaner air from aloft (see also Fig. 1). Figures 6 and 8 present radiation, [NO], [NO_x], and [CO] obtained on 20 and 24 July 2001, respectively, each of which shows the NO_x peak beginning in the 04:00–05:00 EST time frame. If combustion was the source of the NO_x in these cases, there would have been a simultaneous increase in CO of ~30–90 ppb, given the typical value for the CO emission factor of $\Delta CO/\Delta NO_x$ ~8 from mobile sources (McGaughey et al., 2004), and ~25 in stationary source combustion plumes (Neuman et al., 2009; Nicks et al., 2003), and the relatively longer lifetime for CO. While this was not observed, the variability in the CO data is at the lower end of this range, and it is thus difficult to rule that out. For the case shown in Fig. 8, the NO_x peak began roughly one hour before sunrise (clearly before the NO increase). Thus it seems clear that NO_x behaves not at all like O_3 and PAN (species that mix downward upon the breakup of the NBL), but in fact, much more like a species with a surface source, that builds up under the NBL, and is diluted in the surface layer by downward mixing of cleaner air upon breakup of the NBL.

The impact of vertical mixing can also be directly evaluated, using observations of turbulence along with the chemical species. In Fig. 7 we present observations of radiation, calculated friction velocity (a measure of turbulent mixing), NO_x, PAN and ozone concentration data for 20 July 2001. As shown in this figure, while there is a ~3 ppb increase in NO_x starting in the 04:00–05:00 EST time frame, neither PAN nor O_3 increase, as would be expected if the source were downward mixing (Hastie et al., 1993). PAN and O_3 do increase later in the morning as the mixed layer deepens, and PAN and O_3 mix downward (Hastie et al., 1993). The friction velocity is relatively low through the morning NO_x peak. This is further evidence that vertical mixing is not playing a major role since clearly the morning NO_x peak can often occur in very stable conditions.

Along with CO, a number of "markers" of combustion exist that are useful; among them is aerosol. In the summer of 2008 aerosol measurements using an SMPS,

mounted ∼10 m above the canopy on the PROPHET tower were conducted. Figure 9 shows radiation, fine particle number density (15–40 nm diameter range), [NO_x], and O_3 observed on 1 July 2008. As shown in this figure, NO_x begins increasing at ∼04:00, while O_3 is decreasing, presumably a result of dry deposition within the stable boundary layer. At the time of the NO_x peak at ∼7 a.m., there is no significant change in small particle number density, i.e. again no sign of an impact of local combustion-related NO_x. Thus there are numerous cases that clearly do not result from downward mixing of polluted air from aloft, nor from transport of local scale combustion NO_x.

3.3 Upward mixing from surface sources

An alternative possibility is that NO_x from sources below the canopy or soil slowly diffuses upward past the inlet, in the relatively stable night air, and passes the inlet at semi-random times, but enhanced by sunrise-mediated turbulence. Soil NO flux data obtained by Carleton and Carroll (unpublished data, 2003) indicates an upward emission (or flux) in this forest of, on average, ∼180 nmoles m^{-2}-h. If that NO_x mixes into a 40 m layer (i.e. up to roughly the tower inlet height) over a 6 h period (i.e. from sunset to the typical time of observation of the NO_x increase), this is the equivalent of ∼0.7 ppb, within the range of observations. Of course it is more likely that the NO_x emitted would be more stratified and thus the peak concentrations observed as the NO_x-enriched air moves upward past the tower inlet could be greater than this. Thus soil emissions followed by upward mixing could possibly explain a significant amount of the observed NO_x peak. Vertical profile measurements of NO_x conducted in the below-canopy environment in the summer of 2009 are shown in Fig. 10. This plot shows that on average, there is more NO_x at the 34-m height than below, during the early morning hours. Such an average plot can, however, be impacted by occasional transport events carrying large concentrations just above the canopy, as discussed below. Figure 11 is a histogram of the gradients in NO_x for 2009 early morning observations, defined here as ($[NO_x]_{34m}$-$[NO_x]_{6m}$). As shown in Fig. 11, while the mode of the distribution is not significantly different from a no-gradient case, ∼57 % of the time there is a gradient that

would lead to an upward flux of NO_x from the surface. Thus the available information indicates that under stable NBL conditions sufficient NO_x could accumulate under the canopy. If a mixing event were to occur, e.g. a large-scale eddy, then this could account for some of the observations.

3.4 Anthropogenic sources

A last remaining possibility is long-range transport of aged polluted air from anthropogenic sources, e.g., for UMBS, from Detroit or Chicago. A good marker for anthropogenic pollution is toluene, a significant mobile source pollutant. As shown in Fig. 12, on 8 August 1998 there is an increase in NO_x during the time that O_3 is decreasing in the NBL due to dry deposition. Toluene increases with NO_x, in support of the pollution transport hypothesis. In Fig. 13, we show the 24-h. isentropic back trajectory (HYSPLIT) showing that the sampled air likely transported at or very near the surface through the night, with an origin in the Detroit metropolitan area. This suggests that long-range transport of polluted air at or near the surface of the stable NBL may occur. We note that the data shown in Fig. 11 also show instances of gradients with significantly more NO_x at tower height, compared to the surface level. To date, there has been little study of long-range pollutant transport in near-surface stable air. While Banta et al. (1998) discuss that nighttime transport of pollutants away from urban sources is more important than previously thought, the transport is generally thought to occur in the residual layer. In support of this interpretation, examination of the back trajectories (see the Figs. 2S–6S) indicates that all the air masses arriving at the site when the high morning NO_x maximum appeared traveled near the ground and mostly in darkness during the previous 12 h., although the back trajectories are highly uncertain in these cases. While some of the air masses originated or passed through an urban region (Figs. 2S, 4S, 6S), some did not (e.g. Figs. 3S and 5S). The air mass arriving at the site on 20 July 2001 (Figs. 6 and 3S) might have accumulated NO_x from various sources when traveling at low altitude over small towns and highways (Fig. 3S). In contrast, the case of 1 July 2008 (Fig. 9) is difficult to explain by emissions into a

stratified NBL during low-altitude long-distance transport, since the air came from the north over Lake Michigan where there are no significant NO_x sources. It is conceivable that for this case, the soil NO_x flux discussed above was the major factor. It must be that for all nights, transport from upwind sources within the NBL, and the local soil NO_x emissions both contribute, to varying degrees, depending on the source trajectory, and local surface soil conditions (T, soil moisture, etc.).

4 Conclusions

While the morning NO peak is clearly explained by photolysis of NO_2, photochemistry cannot explain the morning peak in NO_x. We showed that this peak is inconsistent with downward mixing from the residual layer, nor can it be caused by photolysis of nitrogen species on the canopy surface, as it often occurs before sunrise. We present data showing that these events likely occur as a result of the lack of vertical mixing during long-range transport of air to the site. During transport the air mass accumulates combustion and/or soil NO_x emissions into the stable NBL. From this work, a picture emerges of a regional surface-bound air mass that "wallows" in the direction of the mean surface wind while accumulating NO_x from the variety of surface sources, both anthropogenic (point and distributed) and natural (likely widely distributed soil emissions), culminating in a peak in [NO_x] just before the NBL breakup with associated downward mixing from the typically lower-NO_x residual layer. Such processes can have a large impact on the composition of the atmosphere prior to and at the time of sunrise, leading to relatively NO_x-rich morning conditions at an otherwise relatively clean-air site. High NO_x levels can impact early morning chemistry involving the NO_3 radical (Reactions R6–R9 below), conversion

$$NO_2 + O_3 \rightarrow NO_3 + O_2 \quad \text{(R6)}$$

$$NO_3 + NO_2 \leftrightarrow N_2O_5 \quad \text{(R7)}$$

$$N_2O_5 + \text{aerosols} \rightarrow \text{aerosol nitrate} \quad \text{(R8)}$$

$$NO_3 + \text{BVOCs} \rightarrow RONO_2 \quad \text{(R9)}$$

of NO_x to HNO_3, and organic nitrates (cf. Perring et al., 2009). Indeed, we find that a very important source of daytime $RONO_2$ production results from NO_3 reaction with isoprene, at the UMBS site (Pratt et al., 2011). There can also be significant impacts on the morning photochemistry, since the enhanced [NO_2] and relatively large relative humidities present at that time can promote HONO production and thus larger OH production rates at sunrise. As chemical transport at night has been little studied, such processes should be investigated further, as part of organized field campaigns. Much light could be shed on this through vertical profile NO_x measurements at night across a sufficient scale (e.g. the Michigan lower peninsula), and through the full boundary layer, as well as high resolution numerical simulations that capture the aforementioned dynamics. Such data, along with regional scale estimates of soil NO_x emissions, can then be used to evaluate and improve regional scale air quality models, such as CMAQ (cf. Smith and Mueller, 2011), to better represent the sunrise to noon component of regional photochemical oxidant evolution, which is clearly impacted by nighttime surface-level NO_x emission and transport. The proper treatment of the behavior of the surface level NO_x in the nighttime and morning periods will require better understanding of mixing and transport in the stable nighttime boundary layer, which is a challenge that may need to include processes such as canopy-atmosphere coupling, not normally treated in models of boundary layer turbulence (Steiner et al., 2011).

Supplementary material related to this article is available online at: http://www.atmos-chem-phys-discuss.net/11/29251/2011/acpd-11-29251-2011-supplement.pdf.

Acknowledgements. We (PBS) gratefully acknowledge support by the National Science Foundation grant, No. ATM0542701, and EPA (STAR Grant R833750).

References

Apel, E. C., Riemer, D. D., Hills, A., Baugh, W., Orlando, J., Faloona, I., Tan, D., Brune, W., Lamb, B., Westberg, H., Carroll, M. A., Thornberry, T., and Geron, C. D.: Measurement and interpretation of isoprene fluxes and isoprene, methacrolein, and methyl vinyl ketone mixing ratios at the PROPHET site during the 1998 Intensive, J. Geophys. Res., 107, D3, 4034, doi:10.1029/2000JD000225, 2002.

Banta, R. M., Senff, C. J., White, A. B., Trainer, M., McNier, R. T., Valente, R. J., Mayor, S. D., Alvarez, P. J., Michael Hardesty, R., Parrish, D., and Fehsenfeld, F. C.: Daytime buidup and nighttime transport of urban ozone in the boundary layer during a stagnation episode, J. Geophys. Res., 103, D17, 22, 519–22,544, 1998.

Carroll, M. A., McFarland, M., Ridley, B. A., and Albritton, D. L.: Ground-based nitric oxide measurements at Wallops Island Virginia, J. Geophys. Res., 90, 12, 12,853–12,860, 1985.

Carroll, M. A., Shepson, P. B., and Bertman, S. B.: Overview of the Program for Research on Oxidants: PHotochemistry, Emissions, and Transport (PROPHET) Summer 1998 Measurements Intensive, J. Geophys. Res., 106, 24,275–24,288, 2001.

Costa, A. W., Michalski, G., Alexander, B., and Shepson, P. B.: Analysis of Atmospheric Inputs of Nitrate to a Temperate Forest Ecosystem from $\Delta^{17}O$ Isotope Ratio Measurements, Geophys. Res. Lett., 38, L15805, doi:10.1029/2011GL047539, 2011.

Day, D. A., Farmer, D. K., Goldstein, A. H., Wooldridge, P. J., Minejima, C., and Cohen, R. C.: Observations of NOx, $\sum$PNs, $\sum$ANs, and HNO_3 at a Rural Site in the California Sierra Nevada Mountains: summertime diurnal cycles, Atmos. Chem. Phys., 9, 4879–4896, doi:10.5194/acp-9-4879-2009, 2009.

Dentener, F. J. and Crutzen P. J.: A 3-dimensional model of the global ammonia cycle, J. Atmos. Chem., 19, 331–369, 1994.

Fehsenfeld, F. C., Drummond, J. W., Roychowdhury, U. K., Galvin, P. J., Williams, E. J., Buhr, M. P., Ridley, B. A., Grahek, F., Heikes, B. G., Kok, G. L., Shetter, J. D., Walega, J. G., Elsworth, C. M., Norton, R. B., Fahey, D. W., Murphy, P. C., Hovermale, C., Mohnen, V. A.,

Demerjian, K. L., and Mackay, G. L.: Intercomparison of NO_2 measurement techniques, J. Geophys. Res., 95, 3579-3597, 1990.

Finlayson-Pitts, B. J., Wingen L. M., Sumner, A. L., Syomin, D., and Ramazan, K. A.: The heterogeneous hydrolysis of NO_2 in laboratory systems and in outdoor and indoor atmospheres: An integrated mechanism, Phys. Chem. Chem. Phys, 5, 223 – –242, 2003.

Galloway, J. N., Townsend, A. R., Erisman, J. W., Bekunda, M., Cai, Z., Freney, J. R., Martinelli, L. A., Seitzinger, S. P., and Sutton, M. A.: Transformation of the nitrogen cycle: Recent trends, questions, and potential solutions, Science, 320, 889–892, 2008.

Gough, C. M., C. S. Vogel, K. H. Harrold, George, K., and Curtis, P. S.: The legacy of harvest and fire on ecosystem carbon storage in a north temperate forest, Glob. Change Biol., 13, 1935–1949, 2007.

Hastie, D. R., Shepson, P. B., Berman, R. and Sharma, S.: The Influence of the Nocturnal Boundary Layer on the Concentration of Secondary Trace Species at Dorset, Ontario, Atmos. Environ., 27*A*, 533–541, 1993.

Kondo, Y., Ziereis, H., Koike, M., Kawakami, S., Gregory, G. L., Sachse, G. W., Singh, H. B., Davis, D. D., and Merrill, J. T.: Reactive nitrogen over the Pacific Ocean during PEM-West A, J. Geophys. Res., 101, 1809–1828, 1996.

Kley, D. and McFarlan, M.: Chemiluminescence detector for NO and NO_2, Atmos. Technol., 12, 63–69, 1980.

Lin, X., Trainer, M., and Liu, S. C.: On The Nonlinearity Of The Tropospheric Ozone, J. Geophys. Res., 93, 15879–15888, 1988.

Lockwood, A. L., Filley, T. R., Rhodes, D., and Shepson, P. B.: Foliar uptake of atmospheric organic nitrates, Geophys. Res. Lett., 35, L15809, doi:10.1029/2008GL034714, 2008.

Magnani, F., Mencuccini, M., Borghetti, M., Lankreijer, H., Law, B. E., Lindroth, A., Lousta, D., Manca, G., Moncrieff, J. B., Rayment, M., Tedeschi, V., Valentini, R., and Grace, J.: The human footprint in the carbon cycle of temperate and boreal forests, Nature, 447, 848–852, 2007.

Martin, R. S., Westberg, H., Allwine, E., Ashman, L., Farmer, J. C., and Lamb, B.: Measurement of isoprene and its atmospheric oxidation products in a central Pennsylvania Deciduous Forest, J. Atmos. Chem., 13, 1–32, 1991.

McGaughey, G. R., Desai, N. R., Allen, D. T., Seila, R. L., Lonneman, W. A., Fraser, M. P., Harley, R. A., Pollack, A. K., Ivy, J. M., and Price, J. H.: Analysis of motor vehicle emissions in a Houston tunnel during the Texas Air Quality Study 2000, Atmos. Environ., 38, 3363–

3372, 2004.
Neuman, J. A., Nowak, J. B., Zheng, W., Flocke, F., Ryerson, T. B., Trainner, M., Holloway, J. S., Parrish, D. D., Frost, G., J., Peischl, J., Atlas, E. L., Bahreini, R., Wollny, A. G., and Fehsenfeld, F. C.: Relationship between photochemical ozone production in Houston, Texas. J. Geophys. Res., 114, D00F08, doi:10.1029/2008JD011688, 2009.
The Nicks et al. authors are: Nicks Jr, D. K., Holloway, J. S., Ryerson, T. B., Dissly, R. W., Parrish, D. D., Frost, G. J., Trainer, M., Donnelly, S. G., Schauffler, S., Atlas, E. Z., Hbler, G, Sueper, D. T., and Fehsenfeld, F. C. : Fossil-fueled power plants as a source of atmospheric carbon monoxide. J. Environ. Monit., 5, 35–39, 2003.
Norby, R. J., Warren, J. M., Iversen, C. M., Medlyn, B. E., and McMurtrie, R. E.: CO_2 enhancement of forest productivity constrained by limited nitrogen availability, Proc. Nat. Acad. Sci., available at: www.pnas.org/cgi/doi/10.1073/pnas.1006463107, 2010.
Ollinger, S. V., Aber, J. D., Reich, R. B., and Freuder, R. J.: Interactive effects of nitrogen deposition, tropospheric ozone, elevated CO_2 and land use history on the carbon dynamics of northern hardwood forests, Global Change Biol., 8, 545–562, 2002.
Penner, J. E., Atherton, C. S., Dignon, J., Ghan, S. J., Walton, J. J., and Hameed, S.: Tropospheric Nitrogen - A 3-Dimensional Study Of Sources, Distributions, And Deposition, J. Geophys. Res., 96, 959–990, 1991.
Perring, A. E., Wisthaler, A., Graus, M., Wooldridge, P. J., Lockwood, A. L., Mielke, L. H., Shepson, P. B., Hansel, A., and Cohen, R. C.: A product study of the isoprene + NO_3 reaction, Atmos. Chem. Phys., 9, 4945–4956, doi:10.5194/acp-9-4945-2009, 2009.
Pippin M. R., Thornberry, T. D., Town, M. S., Carroll, M. A., and Sillman, S.: Seasonal variations of PAN, PPN, and O3 at the upper Midwest PROPHET site. J. Geophys. Res., 106, 24451–24465, 2001.
Parrish, D. D., Buhr, M. P., Trainer, M., Norton, R. B., Shimshock, J. P., Fehsenfeld, F. C., Anlauf, K. G., Bottenheim, J. W., Tang, Y. Z., Wiebe, H. A., Roberts, J. M., Tanner, R. L., Newman, L., Bowersox, V. C., Olszyna, K. J., Bailey, E. M., Rodgers, M. O., Wang, T., Berresheim, H., Roychowdhury, U. K., and Demerjiani, K. L.: The total reactive oxidized nitrogen levels and the partitioning between the individual species at six rural sites in eastern north America, J. Geophys. Res., 98, 2927–2939, 1993.
Pratt, K. A., Mielke, L. H., Shepson, P. B., Bryan, A. M., Steiner, A. L., Ortega, J., Helmig, D. Contribution of individual biogenic volatile organic compounds to organic nitrate formation above a mixed forest, Atmos. Chem. Phys., in preparation, 2011.

Ridley, B. A. and Grahek, F. E., Small, A.: Low Flow, High-Sensitivity Reaction Vessel For NO Chemiluminescence Detectors, J. Atmos. and Ocean. Technol., 7, 307–311, 1990.
Ridley, B. A. and Howlett, L. C., An instrument for nitric oxide measurements in the stratosphere, Rev. Sci. Instrum., 45, 742–746, 1974.
Ridley, B. A., Carroll, M. A., and Gregory, G. L.: Measurements of nitric oxide in the boundry layer and free troposphere over the pacific., J. Geophys. Res., 92, 12, 2025–2047, 1987.
Ridley, B. A., Shetter, J. D., Walega, J. G., Madronich, S., Elsworth, C. M., Grahek, F. E., Fehsenfeld, F. C., Norton, R. B., Parrish, D. D., Hübler, G., Buhr, M., Williams, E. J., Allwine, E. J., and Westberg, H. H.: The behavior of some organic nitrates at Boulder and Niwot Ridge, Colorado, J. Geophys. Res., 95, 13949–13961, 1990.
Ridley, B. A., Madronic, S., Chatfield, R. B., Walega, J. G., Shetter, R. E., Carroll, M. A., and Montzka, D. D.: Measurements and Model Simulations of the Photostationary State During the Mauna Loa Observatory Photochemistry Experiment: Implications for Radical Concentrations and Ozone Production and Loss Rates, J. Geophys. Res., 97, 10375–10388, 1992.
Rollins, A. W., Smith, J. D., Wilson, K. R., and Cohen, R. C.: Real Time In Situ Detection of Organic Nitrates in Atmospheric Aerosols, Environ. Sci. Technol., 44, 5540–5545, 2010.
Sakamaki, F., Hatakeyama, S., and Akimoto, H.: Formation Of Nitrous-Acid And Nitric-Oxide In The Heterogeneous Dark Reaction Of Nitrogen-Dioxide And Water-Vapor In A Smog Chamber, Int. J. Chem. Kinet., 15, 1013–1029, 1983.
Singh, M. P., Mcnider, R. T., and Lin, J. T.: An Analytical Study Of Diurnal Wind- Structure Variations In The Boundary-Layer And The Low-Level Nocturnal Jet, Bound.-Lay. Meteorol., 63, 397–423, 1993.
Smith, S. N. and Mueller, S. F.: Modeling natural emissions in the Community Multiscale Air Quality (CMAQ) Modell: building an emissions data base, Atmos. Chem. Phys., 10, 4931–4952, doi:10.5194/acp-10-4931-2010, 2010.
Steiner, A. L., Pressley, S. N., Botros, A., Jones, E., Chung, S. H., and Edburg, S. L.: Analysis of coherent structures and atmosphere-canopy coupling strength during the CABINEX field campaign: implications for atmospheric chemistry, Atmos. Chem. Phys. Discuss., 11, 21013–21054, doi:10.5194/acpd-11-21013-2011, 2011.
Thompson, A. M.: The Oxidizing Capacity Of The Earths Atmosphere – Probable Past And Future Changes, Science, 256, 1157–1165, 1992.
Thornberry T., Carroll, M. A., Keeler, G. J., Silman, S., Bertman, S. B., Pippin, M. R., Ostling,

K., Grossenbacher, J. W., Shepson, P. B., Cooper, O. R., Moody, J. L., and Stockwell, W. R.: Observation of reactive oxidized nitrogen and speciation of NO_y during the PROPHET summer 1998 intensive, J. Geophys. Res., 106, 24359–24386, 2001.

Wildt, J., Kley, D., Rockel, A., Rockel, P., and Segschneider, H. J.: Emission of NO from several hgher plant species. J. Geophys. Res., 12, D5, 5919–5927, 1997.

Zhou, X., Civerolo, K., Dai, H., Huang, G., Schwab, J., and Demerjian, K.: Summertime nitrous acid chemistry in the atmospheric boundary layer at a rural site in New York State, J. Geophys. Res., 107, 4590, doi:10.1029/2001JD001539, 2002.

Zhou, X. L., Zhang, N., TerAvest, M., Hou, J., Tang, D.,. Bertman, S, Alaghmand, M., Shepson, P. B., Carroll, M. A., Griffith, S., and Stevens, P.: Nitric Acid Photolysis on the Forest Canopy Surface as a Tropospheric Nitrous Acid Source, 4, 440–443, doi:10.1038/NGEO1164, Nat. Geosci., 2011.

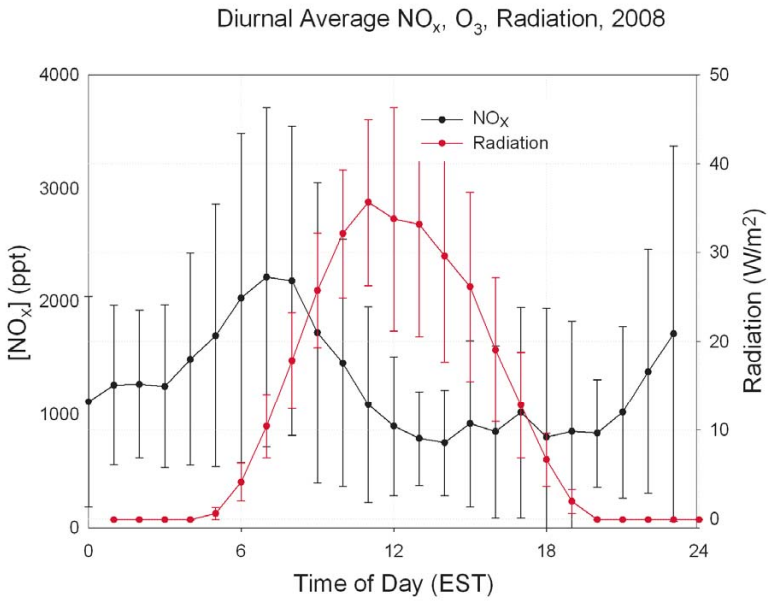

Fig. 1. Diurnal variation of NO_x from 24 June through 26 July 2008 at the PROPHET site and the morning NO_x peak observation.

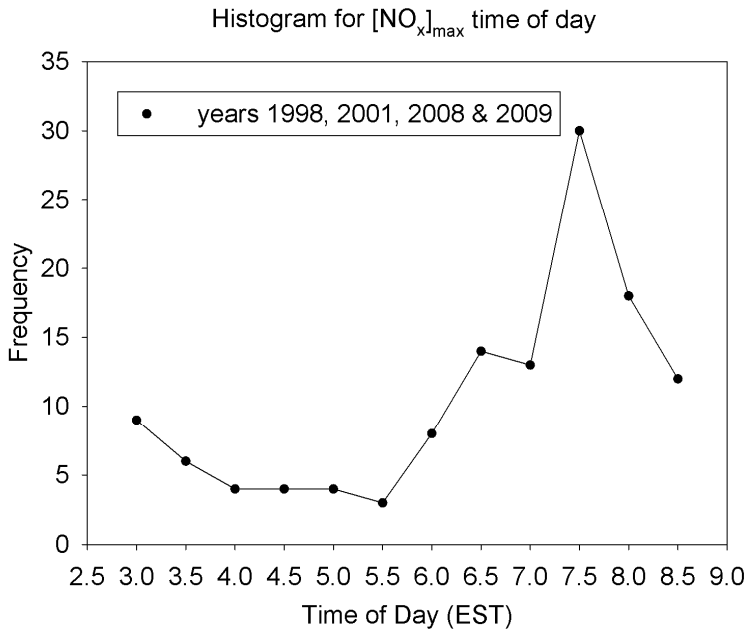

Fig. 2. Histogram of frequency of time of day for maximum NO_x.

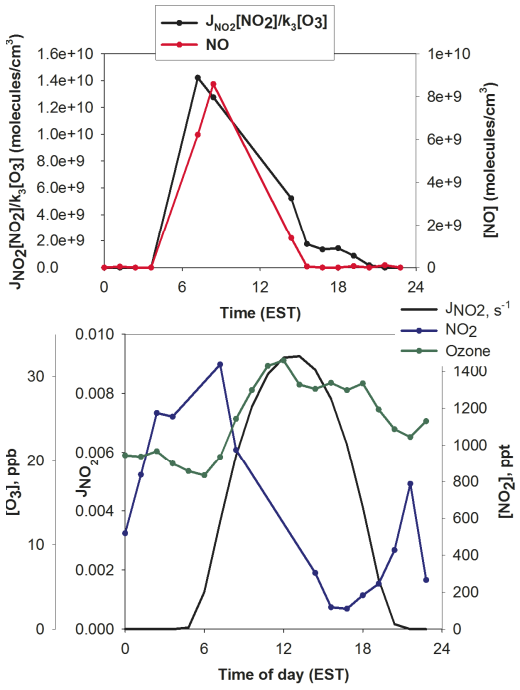

Fig. 3. Observed NO, NO_2 and ozone concentrations, and calculated steady-state NO, for 2 July 2008.

Discussion Paper | Discussion Paper | Discussion Paper | Discussion Paper |

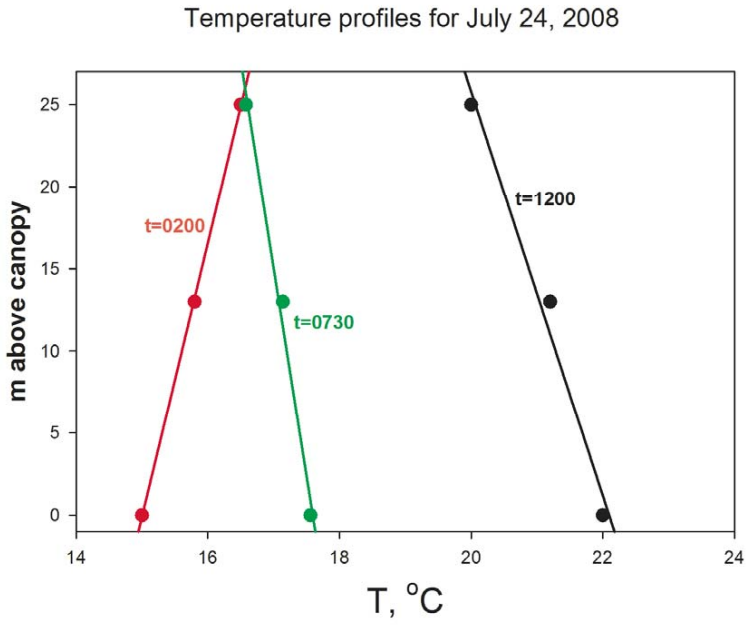

Fig. 4. Temperature Vertical Profiles above the Canopy for 24 July 2008.

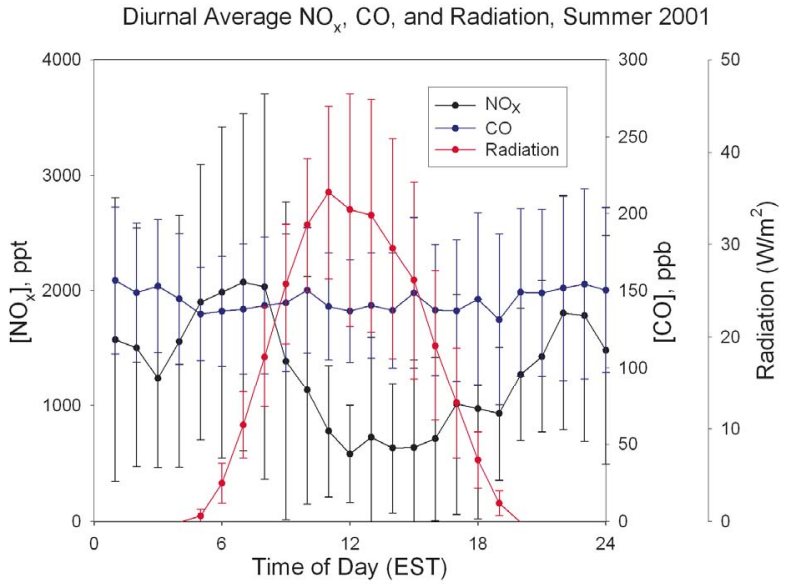

Fig. 5. Diurnal variation of CO, NO_x and radiation observed in summer 2001 at the PROPHET site.

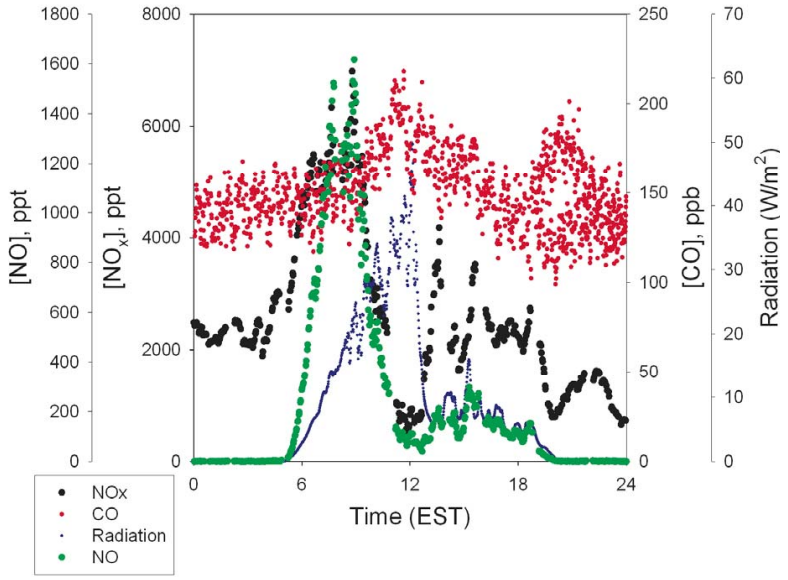

Fig. 6. Time series of radiation, NO, NO_x and CO for 20 July 2001.

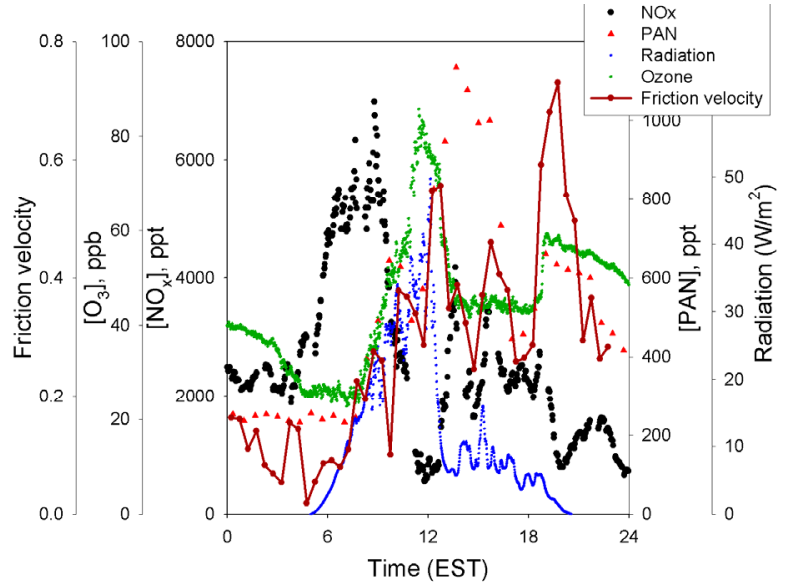

Fig. 7. Observed radiation, friction velocity, $[NO_x]$, [PAN] and $[O_3]$ for 20 July 2001.

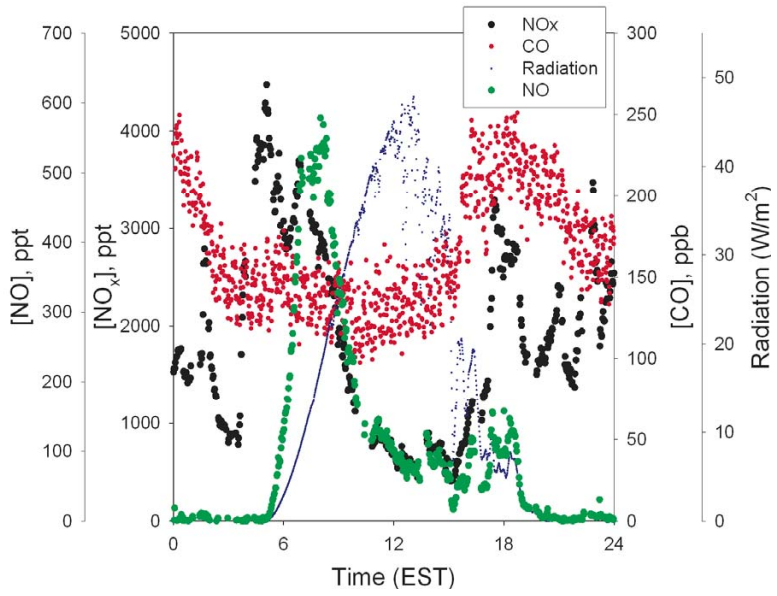

Fig. 8. Time series of radiation, NO, NO_x and CO for 24 July 2001.

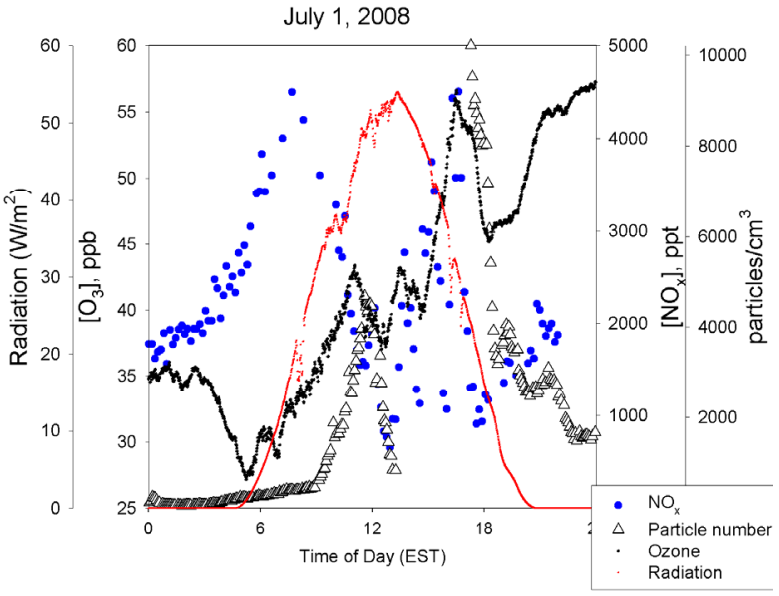

Fig. 9. Radiation, particle number density, $[NO_x]$ and $[O_3]$ observed on 1 July 2008.

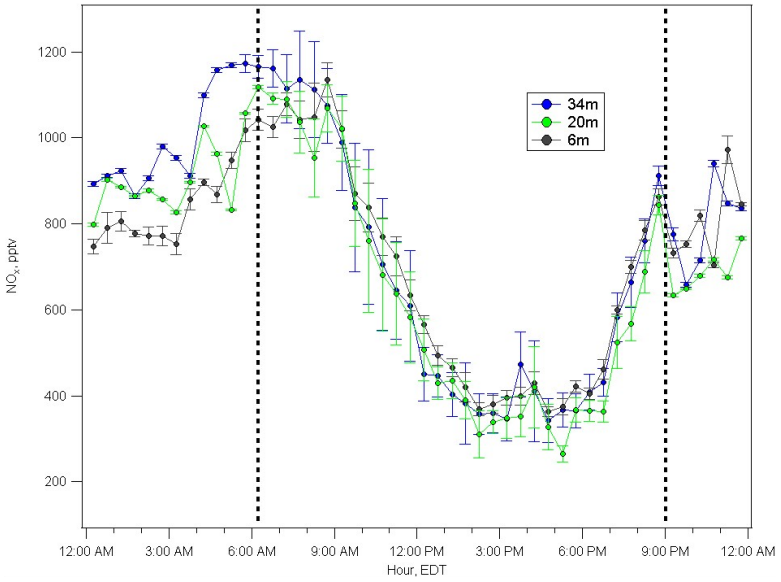

Fig. 10. Diurnal variation of NO_x concentration at three levels (above and below the canopy) observed in summer 2009 at the PROPHET site.

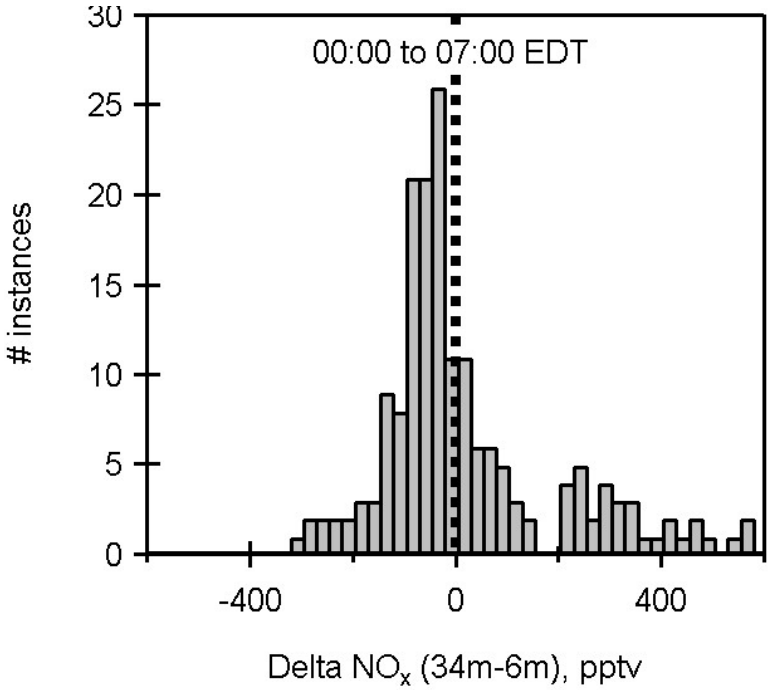

Fig. 11. Histogram for the frequency of the magnitude of the NO_x concentration gradient between 34m and 6m above ground level, during early morning hours, summer 2009.

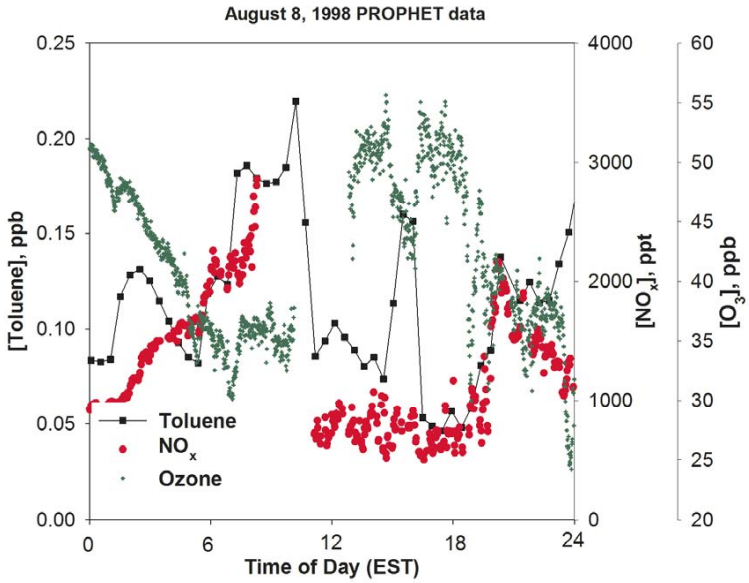

Fig. 12. [Toluene], [NO_x] and [O_3] observed on 8 August 1998.

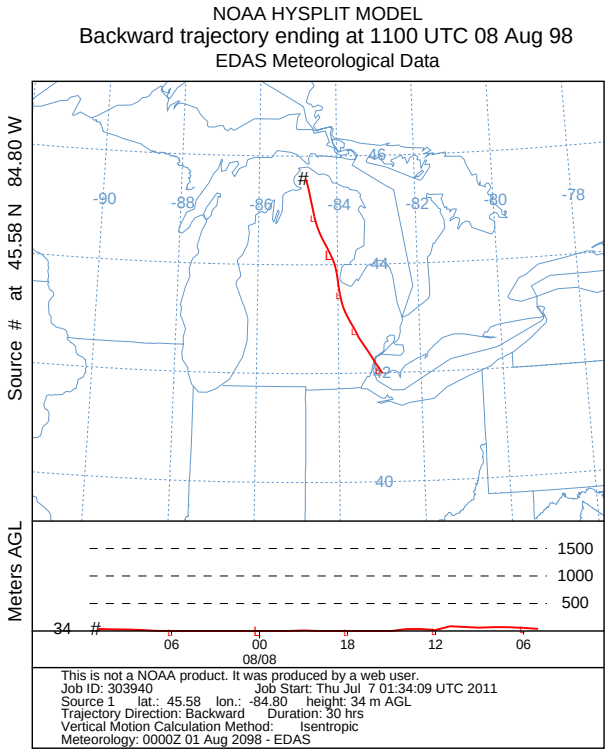

Fig. 13. 24-h. back trajectory for the early morning of 8 August 1998.